Australian Earthquake Engineering Society 2011 Conference, 18-20 November,
Barossa Valley, South Australia

Collapse Limit State Assessment of Lightly Reinforced Concrete Columns

Mohammad Fardipour[1*] and Nelson Lam[1]
Emad Gad[2] and John Wilson[2]

1. Department of Infrastructure Engineering, The University of Melbourne, Victoria
   Email: *mfa@pgrad.unimelb.edu.au
2. Faculty of Engineering and Industrial Sciences, Swinburne University of Technology, Hawthorn, Victoria

Abstract

A range of lightly-reinforced, poorly-confined RC columns were assessed for seismic safety based on the limit state of collapse in projected earthquake scenarios representative of the average level of seismicity in Australia. The hysteresis model for each of the columns analysed were first calibrated against results from cyclic tests and push over analyses up to the limit of gravity collapse. Inelastic time history analyses employing 40 spectrum compatible accelerograms on class C sites (AS 1170.4) were then conducted on the calibrated models. Fragility curves have also been constructed in accordance with results from incremental dynamic analyses. Results presented provide the basis for realistic seismic collapse assessment of the poorly confined reinforced concrete columns. Importantly, the size effects phenomenon has been revealed in this study.

Keywords: Seismic collapse assessment, inelastic dynamic analysis, non-ductile RC columns, axial failure limit

1. Introduction

This paper is concerned with the seismic collapse assessment of lightly reinforced, poorly confined reinforced concrete columns which are commonly seen in soft-storey buildings in Australia. Such columns are conventionally known as non-ductile and are automatically deemed to be unsafe in accordance with code provisions originally developed for conditions of high seismic regions (e.g. ATC-40 (1996), FEMA356 (2000), ASCE/SEI 41-06 (2007)). However, recent studies on ground motion behaviour in regions of low and moderate seismicity (such as Australia) and the displacement capacity of lightly reinforced columns have revealed potentials for a refined and more realistic displacement-based seismic collapse assessment of the columns.

Studies by Lam and Chandler (2005) and Lam and Wilson (2004) on displacement controlled phenomenon revealed that the displacement demand of an elastic single degree of freedom system (SDOF) does not increase indefinitely with the natural period of the system. In other words there is a cap on the elastic displacement demand value in cases where the natural period of the structure exceeds the dominant period of excitations (T_2). Significantly, this peak displacement demand (PDD) phenomenon is applicable to both elastic and inelastic systems. Thus, a lumped mass system experiencing strength and stiffness degradation (hence lengthening of the effective natural period) would also be capped on its displacement demand. It was revealed by the comprehensive study by Lumantarna et al (2010) that this hypothesis is generally true in conditions of low and moderate seismicity. Meanwhile, recent experimental observations revealed surprising level of drift capacity for shear critical RC columns up to the axial load carrying capacity limit (Rodsin, 2008, Wilson *et al.*, 2009, Wibowo *et al.*, 2010b). Importantly it was observed that the axial load carrying capacity of the column would not necessarily be compromised by initial shear distress (and consequential decrease in lateral strength). For RC columns with minimal vertical and transverse bar ratios of the order of 0.5% and 0.07% the reported drift capacity limit (at axial failure) was 1.5% to 5% respectively (Wibowo *et al.,* (2010b).

This paper presents results of a study over the seismic collapse behaviour of lightly RC columns recognizing its reserved additional lateral displacement capacity. An axial capacity model is presented in Section 2 for estimating the drift capacity of RC columns at the limit of gravity collapse. Section 3 contains a brief description of the FE model employed for simulating the force-displacement response behaviour of RC columns. Some details of the input ground motions for time history analyses have also been presented. Section 4 presents results of parametric studies and illustrates the column size effect phenomenon. Factor of safety values derived from the displacement-based approach are then compared against values derived from the conventional force-based approach. Section 5 presents results of incremental dynamic analyses in the form of fragility curves.

2. Axial drift capacity model

This section presents an axial drift capacity model for shear critical columns that experience yielding of longitudinal bars prior to experiencing excessive shear deformation leading to collapse. A shear mode of failure featuring very brittle behaviour without yielding of any longitudinal reinforcement) may occur in overly reinforced columns with low shear span to depth ratio and is beyond the scope of this paper. The proposed capacity model is a

modified/supplemented version of the model proposed by Elwood and Moehle (2005) and has been validated against column specimens that were tested at Chulalongkorn University in Thailand forming part of the collaboration with Swinburne University of Technology and University of Melbourne. The tested cantilever columns (S1- to S4) had dimensions of $270\times300\times1200$, moderate axial load ratio of 20% to 40 %, a nominal transverse bar ratio of 0. 07% ($\phi6$ @ 300 mm) and vertical bar ratio of 0.5% to 1%. Refer to publications by the authors (Wibowo *et al.*, 2010b, 2010a) for detailed descriptions of the column specimens, test set up and experimental observations.

2.1. Drift capacity model proposed by Elwood and Moehle (2005)

In the capacity model proposed by Elwood and Moehle, all axial loads supported by a shear damaged column must be transferred across the shear failure plane through a mechanism known as shear – friction which is function of the normal stresses applied onto the crack surface. These normal stresses are resulted from (i) the elongation of the transverse and longitudinal reinforcements crossing the crack surface and (ii) gravity load on the column resolved in the direction perpendicular to the crack surface (Figure 1). Axial load failure (ie gravity collapse) is imminent as the shear friction demand exceeds the shear-friction resistance limit on the crack surface. A sudden drop in the frictional resistance can be resulted from softening of the transverse bars, opening of the shear crack and crushing of concrete at the reduced contact area.

Elwood and Mohele based their analyses on the equilibrium of forces at the critical crack plane (as shown in Figure 1) and proposed Eq.1 for estimating the drift ratio (Δ / L) at axial failure as a function of a number of key parameters: namely axial load (P), transverse bar area (A_{st}), transverse bar yield strength (f_{yt}), spacing of stirrups(s) and d_c which is the distance from centreline to centreline of vertical bars.

$$\left(\frac{\Delta}{L}\right)_{axial} = \frac{4}{100}\frac{1+(\tan\theta)^2}{\tan\theta + P\left(\dfrac{s}{A_{st} f_{yt} d_c \tan\theta}\right)} \quad \textbf{(1)}$$

An empirical trend line (Eq.2) has also been proposed for estimating the critical crack angle θ as a function of the axial load ratio (P/P_0). θ values were obtained from direct measurement of the observed critical crack angles of the corresponding columns.

$$\theta = 55 + 35P/P_0 \quad \text{where} \quad \textbf{(2)}$$

$$P_0 = 0.85 f_c^{'}(A_{g-}A_{sl}) + f_{yl}A_{sl} \quad \textbf{(3)}$$

where P_0 is the axial capacity of the undamaged column, $f_c^{'}$ is the concrete compressive strength, A_g is the gross area of column cross section, A_{sl} is the area of longitudinal steel and f_{yl} is the yield strength of longitudinal reinforcement.

In deriving Eq.1 the following steps were taken :

1. Equations of equilibrium in horizontal and vertical directions were written to incorporate resolved components of forces acting on the critical shear crack (Figure 1). Dowel actions of the longitudinal bars (V_s) were excluded given its reported limited effects.

2. With reference to the classical shear friction model, the unknown shear resistance force V_{sf} was replaced by the product of the effective coefficient of friction μ and compression force (N) which acts in the direction normal to that of the crackline.
3. Algebraic manipulations of the equations of equilibrium resulted in an expression for estimating μ as functions of the amount of transverse reinforcement, axial load (P) and critical crack angle θ (Eq 4). The value of the external shear force (V) has been set to zero given that the shear (lateral) capacity is negligible when approaching axial failure.

$$\mu = \frac{P - A_{st} f_{yt} d_c / s}{P / \tan\theta + A_{st} f_{yt} d_c \tan\theta / s} \quad \textbf{(4)}$$

4. μ values were then estimated using equation (4) for each of the 12 columns included in the dataset. In these calculations an average critical crack angle ($\theta = 65^\circ$) was assumed for all the columns.
5. The calculated μ values were then plotted against total drift ratios at axial failure (Δ / L) as obtained experimentally (Figure 3). The trend displayed by the figure could be represented by Eq.5.

$$\mu = \tan\theta - \frac{100}{4}\left(\frac{\Delta}{L}\right)_{Axial} \geq 0 \quad \textbf{(5)}$$

6. Equation 5 was then substituted back into the unified equilibrium equation (as outlined in Step 3) for estimating the drift ratio at axial failure (Eq.1).

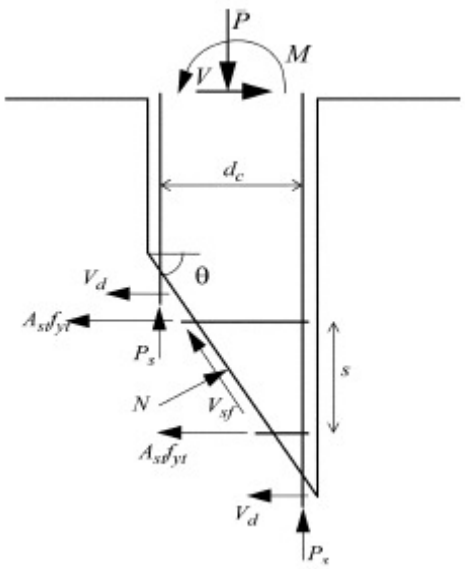

Figure 1. Forces acting at critical shear cracks

Equations 1 to 3 were considered for estimating the ultimate drift capacity of the columns tested in Thailand. The first column (S1), however, was excluded from analyses presented herein as the mode of failure was not dominated by shear. The drift limits of Columns S2-S4 calculated using these equations were found to be significantly exceeded by values observed from the laboratory experiments. Reasons for the discrepancies have been postulated: (i) inclusion of pre-yield displacement in the calibration of the value of the shear friction coefficient (Eq.5, Figure 3) and (ii) errors in estimating the value of θ (ie, $\theta = 65^\circ$ or the values obtained from Eq. 2 for Columns S2 and S3).

2.2. Revision to the estimated angle of critical shear crack

Figure 2.a was taken from Elwood and Moehle (2005) which shows the observed critical crack angles for columns reported in their study. The solid line shown in the figure is the line of best fit as defined by Eq. 2 (given before). Figure 2.b shows similar experimental results observed in this study for Columns S2 to S4 superimposed by the same trend line.

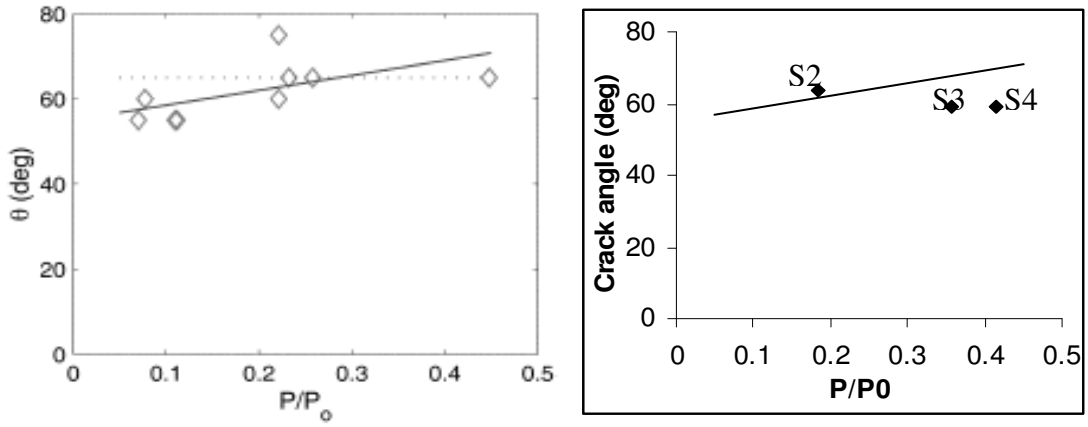

(a) (b)

Figure 2. Correlation of the critical shear crack angle with axial load ratio P/P0 – (a) Results from Elwood and Moehle (2005), (b) Results derived from this study

It can be seen that both sets of experimental data are generally consistent in spite of the fact that the vertical bar ratio of the columns tested in this study was much lower than column specimens reported by Elwood and Moehle (by at least a factor of two). However, it is evident from the experimental data presented in Figures 2a and 2b that the value of the critical crack angle (θ) would not increase indefinitely with the axial load ratios P/P_0 which is contrary to Eq.2. It is proposed herein that Eq 2. is only valid in conditions where $P/P_0 \le 0.25$. For higher values of the axial load ratio, the crack angle may conservatively be taken as a constant value equal to 59 degree. Eq. 2 is accordingly defined as follows:

$$\theta = 55^\circ + 35P/P_0 \quad \text{for} \quad P/P_0 \le 0.25$$
$$\theta = 59^\circ \quad \text{for} \quad P/P_0 > 0.25 \qquad \textbf{(6)}$$

2.3. Revision to the effective coefficient of friction

Elwood and Moehle (2005) introduced the effective coefficient of friction μ (or μ_m) which is function of the total drift ratio Δ/L (as per Eq.5)

It is proposed herein that the effective coefficient of friction μ be related only to the portion of drift in excess of the yield drift ratio (Δ_y/L). This may be justified considering the fact that the formation of a critical shear crack would typically coincide with the occurrence of flexural yielding for lightly confined columns. Thus, the total drift ratio at the limit of axial failure be estimated as the sum of the flexural (yield) drift ratio and the post yield drift ratio as defined by Eq.1.

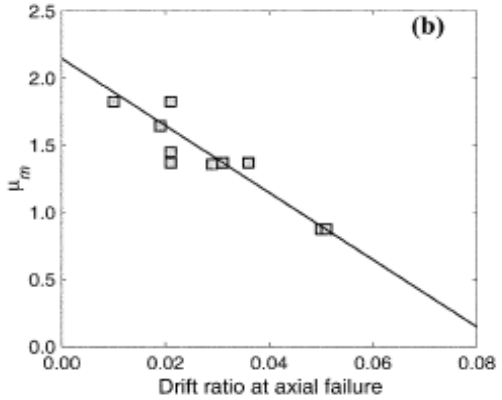

Figure 3 Effective shear friction coefficient vs drift ratio at axial failure
(Elwood and Moehle 2005)

2.4. Revision to yield curvature

Yield curvature is required for estimating yield deformation which may be obtained using a rigorous non-linear section analysis (moment-curvature analysis). Yield curvature ϕ_y may alternatively be obtained by employing the simplified equation proposed by Priestley *et al.* (2007).

$$\phi_y = k\varepsilon_y / d \quad \textbf{(7)}$$

where ε_y is the yield strain , d is the depth of a section and $k = 2.1$ for rectangular RC columns (recognizing that, in general, the value of k is insensitive to the axial load ratio and reinforcement ratio).

However, Figure 4 shows values of $k = \phi_y d / \varepsilon_y$ (obtained from non-linear moment-curvature analyses) for the three sections (A, B & C), with axial load ratios varying in the range: 0.1 - 0.4 and vertical bar ratios varying in the range: 0.5% - 1.5%. The transverse reinforcement ratio was 0.07% for all cases which were characterised by the conditions of un-confinement. The thick dashed line in this figure represents the average trend as represented by Eq.8. It is seen that the mean value of k obtained from analyses (ie. K=2.14) is in good agreement with K=2.1 as recommended by Priestley *et al.* (2007). It is therefore suggested that Eq. 8 be used for the purpose of this study for obtaining refined estimates for the value of the yield curvature and hence yield drift.

$$K = 3\times\rho + 1.4\,, \qquad 0.1 \le \rho \le 0.4 \text{ and} \quad \textbf{(8)}$$

$$\rho = P / A_g f_c^{'} \quad \textbf{(9)}$$

Table 1 presents the estimated drift value at axial failure for the tested columns S2-S4 using the outlined simplified approach (Sections 2.2 to 2.4). This table shows that the estimated ultimate drift capacities are reasonably close to experimental observations.

Table 1. Observed and Estimated drifts at the limit of axial collapse for Columns S2-S4

Column	Observed crack angle	Estimated crack angle **Eq. 4**	Yield drift ratio% **Eqs. 6,7&...**	Post yield drift ratio% **Eq.1**	Estimated drift at gravity collapse%	Observed drift at gravity collapse %
S2	63.4	61.4	0.69	1.25	1.94	2.25
S3	59	59	0.89	0.60	1.5	1.5
S4	59	59	0.91	0.47	1.38	1.5

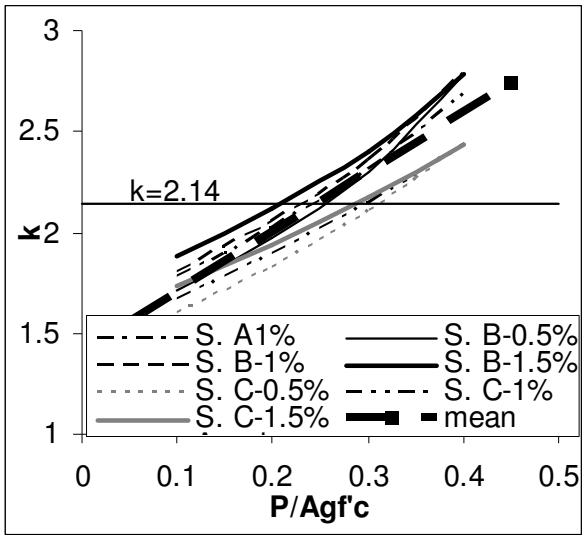

Figure 4. Parameter *K* as a function of axial load ratio (P/Agf'c)
Sections: A(270mm*300mm), B (360*360) and C (540*540)

3. Inelastic time history analysis

Finite element program 'OpenSees' by McKenna et al. (2000) was employed for simulating the force-displacement behaviour of the RC columns of interest. The FE model developed utilizes a non linear beam column element with a hinge at each end. Column nonlinearity is defined at the level of materials and through the input stress-strain relationships for concrete and steel. The element plasticity is distributed within the user-specified hinge length and with the aid of the two integration points implemented at each end. A separately defined fibre section is assigned to each hinge as is required for the built-in nonlinear moment-curvature analysis. This element is therefore capable of including the axial-flexural interaction of stresses. The ultimate drift limit at axial failure however is estimated in accordance with the procedure outlined in Section 2 and is introduced manually.

Figure 5 shows the force-displacement hysteretic response of Column S4. It is shown that the simulated and observed responses are in good agreement. Similar results were obtained for Columns S2 and S3. Consequently, the calibrated FE model was considered reliable for simulating the force-displacement response of similar columns included in the parametric study.

Forty accelerograms on rock sites were generated by stochastic simulations of the seismological model using Program GENQKE as input data required for time history analyses (Lam, 1999, Lam et al., 2000, Lam et al., 2005). These accelerograms represent the design level of excitations expected in Australia for a return period of 500 years (PGV on rock ~ 60mm/s). Different magnitude - distance combinations (M= 5.5-7, R=20-85km) consistent with the design PGV level were considered to account for the random nature of earthquake excitations. Simulated ground motions on rock were then amplified using the well established program, SHAKE, (Idriss and Sun, 1992) to generate representative accelerograms on soil sites. For this purpose three representative boreholes (classified as class C in accordance with AS1170) with initial site periods ranging from 0.25s to0.59 s have been included in the simulations.

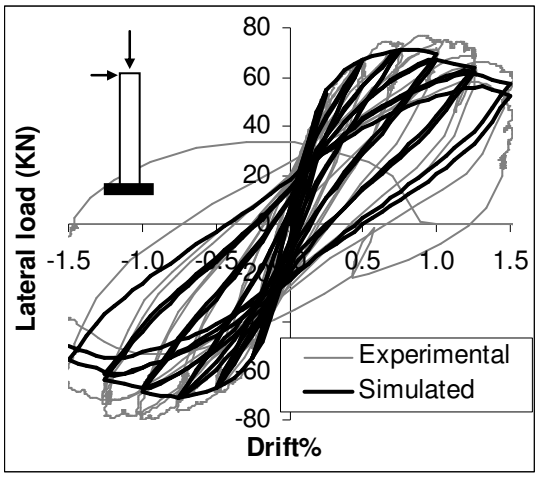

Figure 5. Observed and simulated hysteretic responses for Column S4.

4. Assessment for collapse of columns

Figure 6 presents results of seismic assessment of three columns with a constant square cross section of 450mm*450mm. In this group (Group 1), the height of the columns varied within the range of 2880mm to 4320mm. The axial load ratio was 40%, longitudinal and reinforcement ratio was 1% and transverse reinforcement ratio was 0.07%. Columns were free to sway with a fully fixed connection to the base and rotationally fixed connection to the rest of the structure at the upper end of the column. As can be seen in Figure 6, the average and maximum displacement demands as obtained from 40 inelastic time history analyses are superimposed onto the simulated backbone curve of the corresponding columns. The ultimate point on each backbone curve was estimated using the proposed axial capacity model as described in Section 2.

It was found that the shortest column (SH, with natural period of T=0.4) has the least factor of safety (FOS_{dis} =1.2) in spite of the higher stiffness and lateral force capacity. Factor of safety is calculated herein as the ratio of the column displacement capacity at the limit of gravity collapse and the maximum displacement demand.

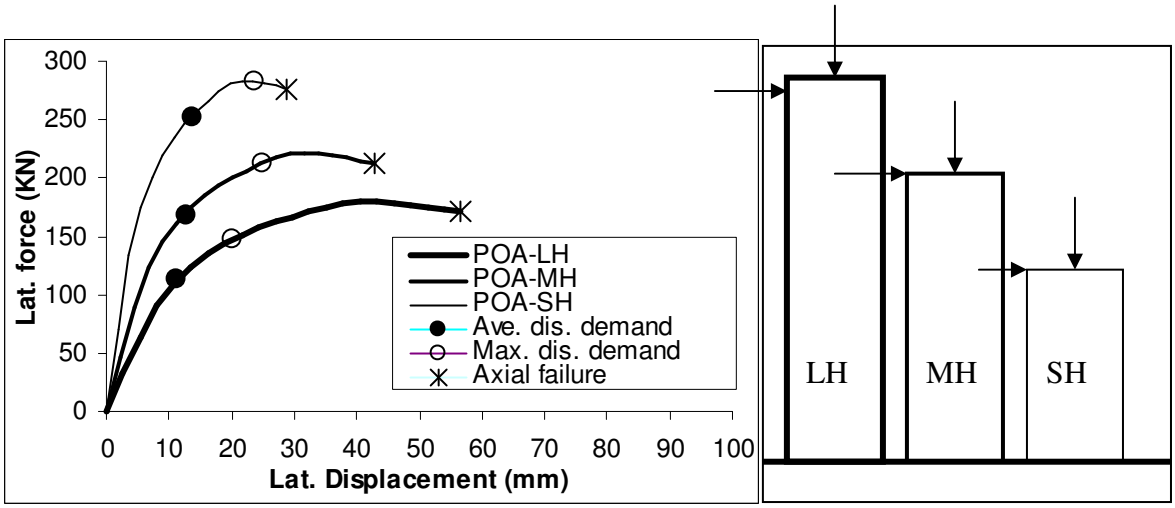

Figure 6. Visualization of the seismic collapse assessment of the columns in Group 1
Height is the only parameter included in this group

It is shown that for a given cross section of the column and material property, the shorter the column the lower the value of the yield displacement capacity and natural period of vibration (because of higher value of $K = 12EI / L^3$). For ground motions on class C sites the peak response spectral displacement would typically peak at a natural period of less than 0.6 second. Thus, the short column (SH) would experience a slightly higher level of displacement demand whilst having the most limited displacement capacity as shown in Figure 6. In contrast, the long column (LH) would be subject to a slightly lower displacement demand whilst having the highest drift capacity, which is translated to a factor of safety $FOS_{dis} = 2.7$. Interestingly, applying the force-based approach would have estimated very different factor of safety (FOS_{force}) values which varied in the range 0.6 - 0.74 implying that the columns would be unsafe in the projected level of earthquake ground shaking (where FOS_{force} is defined as the ratio of lateral load capacity of the column and the seismic shear force demand estimated in accordance with AS1170.4 for PGV value of 60 mm/s on rock).

Figure 7 presents similar results for columns in Group 2 featuring various dimensions but a constant aspect ratio. The medium size column (MD) has the same dimensions as the columns in Group 1. Colmuns LD and SD have been scaled up and down by 25% respectively from the dimension of Column MD. The axial load ratio and reinforcement ratios were kept the same as with columns in Group 1. It was found from inelastic time history analyses of these columns that the value of the seismic displacement demand of each column was well within the respective displacement capacity and with values of FOS_{dis} varying in the range 1.2 - 2 (Figure 7). In contrasts, values of FOS_{force} as derived from the conventional force-based procedure were all less than unity.

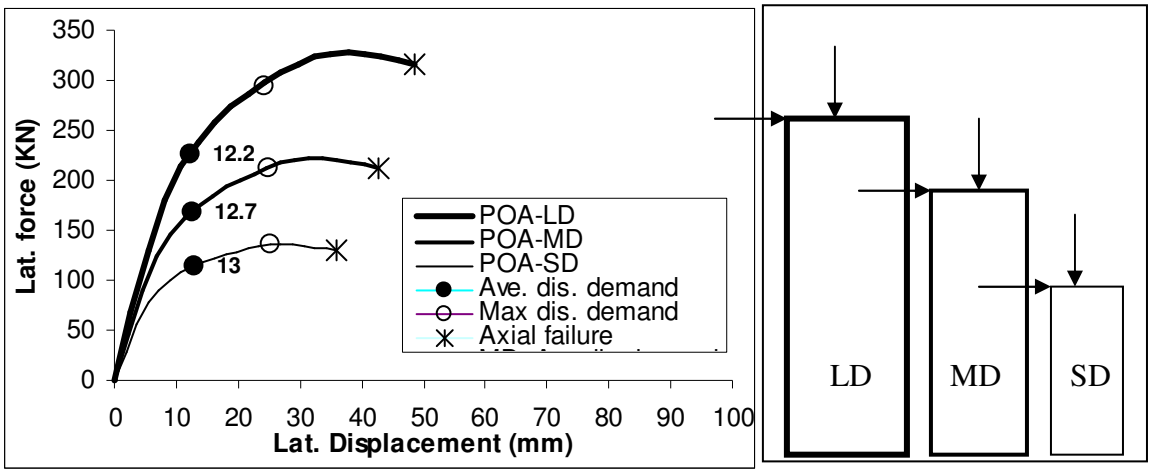

Figure 7 .Visualization of the seismic collapse assessment of the columns in Group 2 Column size is the only parameter included in this group. Aspect ratio is constant

5. Incremental dynamic analysis- Fragility curves

A total of 108 accelerograms on rock (with incremental intensity) were generated using the procedure outlined in Section 3. Nine earthquake scenarios of different magnitude-distance combinations (i.e. M=7, R=10 to 70km) were considered. The accelerograms that have been generated are characterised by peak ground velocity (PGV) values ranging between 34 and 400 mm/s.

Displacement demand values imposed on each of the columns by the incremental ground motions were calculated using inelastic time history analysis (considered columns are addressed in Figures 6 and 7). To identify cases of collapse the calculated demand values were compared against the respective drift capacity values (as calculated using the procedure outlined in Section 2). Fragility curves were then constructed (in accordance with the procedure described by Shinozuka et al (2001)) to correlate the cumulative probability of collapse against maximum response spectral velocity (*RSVmax*) value of the ground shakings.

Results presented in Figure 8 for lightly reinforced RC columns suggest that height is an important parameter affecting the probability of failure of the columns. Column *size* also has significant effect on the probability of failure but of lesser extent compared to *height*. Detailed discussion on trends requires rigorous justification which is beyond the scope of this paper. It is however evident that for a given aspect ratio, axial load ratio and reinforcement ratio, the smaller the dimensions of the column, the higher the probability of collapse.

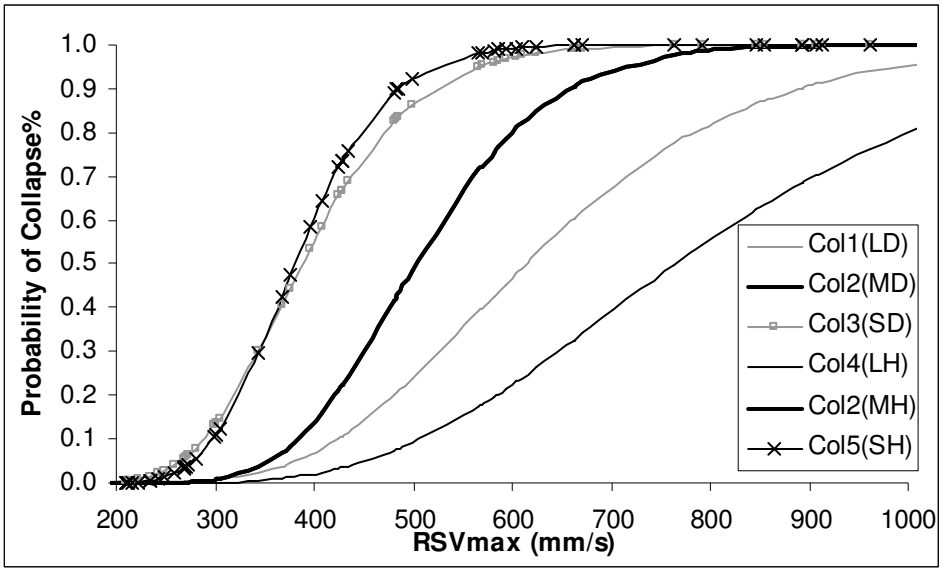

Figure 8. Probability of collapse of lightly reinforced RC columns
(notations in legend - L: large, M: medium, S: Small size, D: dimensions, H: height)

6. Summary and Conclusions

i. An axial capacity model is proposed for estimating the drift capacity of lightly reinforced concrete columns at the limit of gravity collapse (Section 2).

ii. In the proposed axial capacity model, the value of the total drift capacity is calculated as the sum of *yield drift* and *post yield drift* capacity (which can be estimated using Eq.1).

iii. An OpenSees FE model was employed for simulating the force-displacement response behaviour of the lightly reinforced RC columns. The simulated hysteretic models have been calibrated against results obtained from experiments conducted in Thailand.

iv. A range of lightly reinforced ($\rho_l = 1\%$) and poorly confined ($\rho_t = 0.07\%$) RC columns with a high axial load ratio (40%) were then assessed by non-linear time history analyses using the calibrated hysteretic models. The columns were subjected to design-level, spectrum-compatible earthquake excitations (for class C) with incremental intensity.

v. At design level, the calculated factor of safety FOS_{dis} values based on displacement principles were in the range 1.2 to 2.7. In contrasts, FOS_{force} values calculated from conventional force-based procedure were less than unity.

vi. Fragility curves have been constructed to correlate the cumulative probability of collapse of the columns with the maximum response spectral velocity of the earthquake ground motions.

vii. Based on the analyses carried out during this study it was concluded that for a given aspect ratio, axial load ratio and reinforcement ratio, the smaller the dimensions of the column, the higher the probability of collapse.

7. References

ASCE/SEI 2007. Seismic Rehabiliation of Existing Buildings (ASCE/SEI 41-06). Virginia, USA: American Society of Civil Engineers.

ATC 1996. Seismic Evaluation and Retrofit of Concrete Buildings (ATC-40). California, USA: APPLIED TECHNOLOGY COUNCIL.

ELWOOD, K. J. & MOEHLE, J. P. 2005. Axial Capacity Model for Shear-Damaged Columns. *ACI Structural Journal,* 102**,** 578-587.

FEMA 2000. PRESTANDARD AND COMMENTARY FOR THE SEISMIC REHABILITATION OF BUILDINGS (FEMA 356). FEDERAL EMERGENCY MANAGEMENT AGENCY, Washington, D.C.

IDRISS, I. & SUN, J. 1992. Users Manual for SHAKE91. National Institute of Standards and Technology, Maryland, USA and University of California, Davis, USA.

LAM, N. 1999. Program 'GENQKE' user's Guide. Department of Civil & Environmental Engineering, University of Melbourne, Australia.

LAM, N. & CHANDLER, A. 2005. Peak displacement demand of small to moderate magnitude earthquakes in stable continental regions. *Earthquake Engineering & Structural Dynamics,* 34**,** 1047.

LAM, N. & WILSON, J. 2004. DISPLACEMENT MODELLING OF INTRAPLATE EARTHQUAKES. *ISET Journal of Earthquake Technology,* 41**,** 15-52.

LAM, N., WILSON, J. & HUTCHINSON, G. 2000. Generation of synthetic earthquake accelerograms using seismological modelling. *Journal of Earthquake Engineering,* 28**,** 179-195.

LAM, N., WILSON, J. & VENKATESAN, S. 2005. Accelerograms for Dynamic Analysis under the New Australian Standard for Earthquake Actions. *Electronic Journal of Structural Engineering,* 5**,** 10-35.

LUMANTARNA, E., LAM, N., WILSON, J. & GRIFFITH, M. 2010. Inelastic Displacement Demand of Strength-Degraded Structures. *Journal of Earthquake Engineering,* 14**,** 487-511.

MCKENNA, F., FENVES, G. L. & SCOTT, M. H. 2000. Open system for earthquake engineering simulation. Berkeley, Calif. University of California.

PRIESTLEY, M. J. N., CALVI, G. M. & KOWALSKY, M. J. 2007. *Displacement-Based Seismic Design of Structures,* Pavia, ITALY, IUSS Press.

RODSIN, K. 2008. *Seismic performance of soft-storey buildings in low to moderate seismicity regions.* PhD Thesis, University of Melbourne.

SHINOZUKA, M., FENG, M. Q., KIM, H., UZAWA, T. & UEDA, T. 2001. Statistical analysis of fragility curves. Technical Report MCEER, Department of Civil and Environmental Engineering, University of Southern California, Los Angeles, California.

WIBOWO, A., WILSON, J., FARDIPOUR, M., LAM, N., RODSIN, K., LUKKUNAPRASIT, P. & GAD, E. Year. Seismic performance assessment of lightly reinforced concrete columns. *In:* Incorporating Sustainable Practice in Mechanics and Structures of Materials, 2010a Melbourne, Australia. CRC Press, 341-346.

WIBOWO, A., WILSON, J. L., LAM, N. T. K., GAD, E. F., FARDIPOUR, M., RODSIN, K. & LUKKUNAPRASIT, P. Year. Drift capacity of lightly reinforced concrete columns. *In:* Australian Earthquake Engineering Society Conference, 2010 2010b Perth, Australia

WILSON, J., LAM, N. & RODSIN, K. 2009. Collapse Modelling of Soft-storey Buildings. *Australian Journal of Structural Engineering,* 10**,** 11-23.